

The second rainy season onset in the Central Highlands of Vietnam

Ming-Cheng Yen¹, Hai Manh Bui¹, Chi-Ming Peng¹, Yen-Ta Fu¹, Tu Duc Dinh¹, and Neng-Huei Lin¹

¹National Central University

November 26, 2022

Abstract

Two distinct rainfall stages over the Central Highlands (CH) of Vietnam during the rainy season have been objectively defined using the high-resolution Vietnam Gridded Precipitation dataset for 1983–2010 (28 years): a second rainy season (SRS) embedded in the conventional rainy season. Surprisingly, the pronounced interannual variation in the SRS onset date has led to three apparent regimes: an early (late) SRS with a 1 month longer (shorter) rainfall period occurring in early July (until mid-August) and a normal SRS starting in late July. Almost all the early SRS years occur during El Niño developing phases, particularly during the Niño3.4 sea surface temperature (SST) increase from January through December. Water vapor budget analyses reveal that the interannual variation in the divergent water vapor flux is in response to the warmer July tropical Pacific SST anomalies, resulting in rainfall enhancement over the CH and eventually inducing early SRS onset.

Hosted file

supporting information (si).docx available at <https://authorea.com/users/556258/articles/606375-the-second-rainy-season-onset-in-the-central-highlands-of-vietnam>

1 **The second rainy season onset in the Central Highlands of Vietnam**

2
3 **Bui-Manh Hai¹, Chi-Ming Peng^{1,2}, Yen-Ta Fu¹, Duc-Tu Dinh^{1,3}, Neng-Huei Lin¹, and**
4 **Ming-Cheng Yen¹**

5 ¹Department of Atmospheric Sciences, National Central University, Chung-Li, Taiwan.

6 ² WeatherRisk Explore Inc., Taipei, Taiwan.

7 ³ Aero-Meteorological Observatory, Vietnam Meteorological and Hydrological Administration,
8 Hanoi, Vietnam.

9
10 Corresponding author: Ming-Cheng Yen (tyenmc@atm.ncu.edu.tw)

11 **Key Points:**

- 12 • A second rainy season (SRS) is embedded within the conventional rainy season
- 13 • Early (late) SRS with a 1 month longer (shorter) rainfall period occurs in early July (until
- 14 mid-August); a normal SRS starts in late July
- 15 • Almost all the early SRS years occur during El Niño developing phases
- 16
- 17

18 Abstract

19 Two distinct rainfall stages over the Central Highlands (CH) of Vietnam during the rainy season
20 have been objectively defined using the high-resolution Vietnam Gridded Precipitation dataset
21 for 1983–2010 (28 years): a second rainy season (SRS) embedded in the conventional rainy
22 season. Surprisingly, the pronounced interannual variation in the SRS onset date has led to three
23 apparent regimes: an early (late) SRS with a 1 month longer (shorter) rainfall period occurring in
24 early July (until mid-August) and a normal SRS starting in late July. Almost all the early SRS
25 years occur during El Niño developing phases, particularly during the Niño3.4 sea surface
26 temperature (SST) increase from January through December. Water vapor budget analyses reveal
27 that the interannual variation in the divergent water vapor flux is in response to the warmer July
28 tropical Pacific SST anomalies, resulting in rainfall enhancement over the CH and eventually
29 inducing early SRS onset.

30 Plain Language Summary

31 The Central Highlands (CH) of Vietnam contribute up to 90% of the country's total coffee
32 production and 25% of its total hydropower potential. A second rainy season (SRS) is observed
33 in late July in this region, which is distinct from the conventional rainy season that occurs in late
34 April–early May. Because the onset of the SRS has a strong impact on coffee yield and
35 hydropower potential in the CH, this study examines the climatology of and interannual variation
36 in the SRS onset date during 1983–2010. An early (late) SRS with a 1 month longer (shorter)
37 rainfall period occurs in early July (until mid-August). Almost all the early SRS years occur
38 during El Niño developing phases. An association between the early SRS onset years and
39 strengthening of the water vapor flux convergence induced by the warmer July tropical Pacific
40 SST anomalies is discovered.

41 1 Introduction

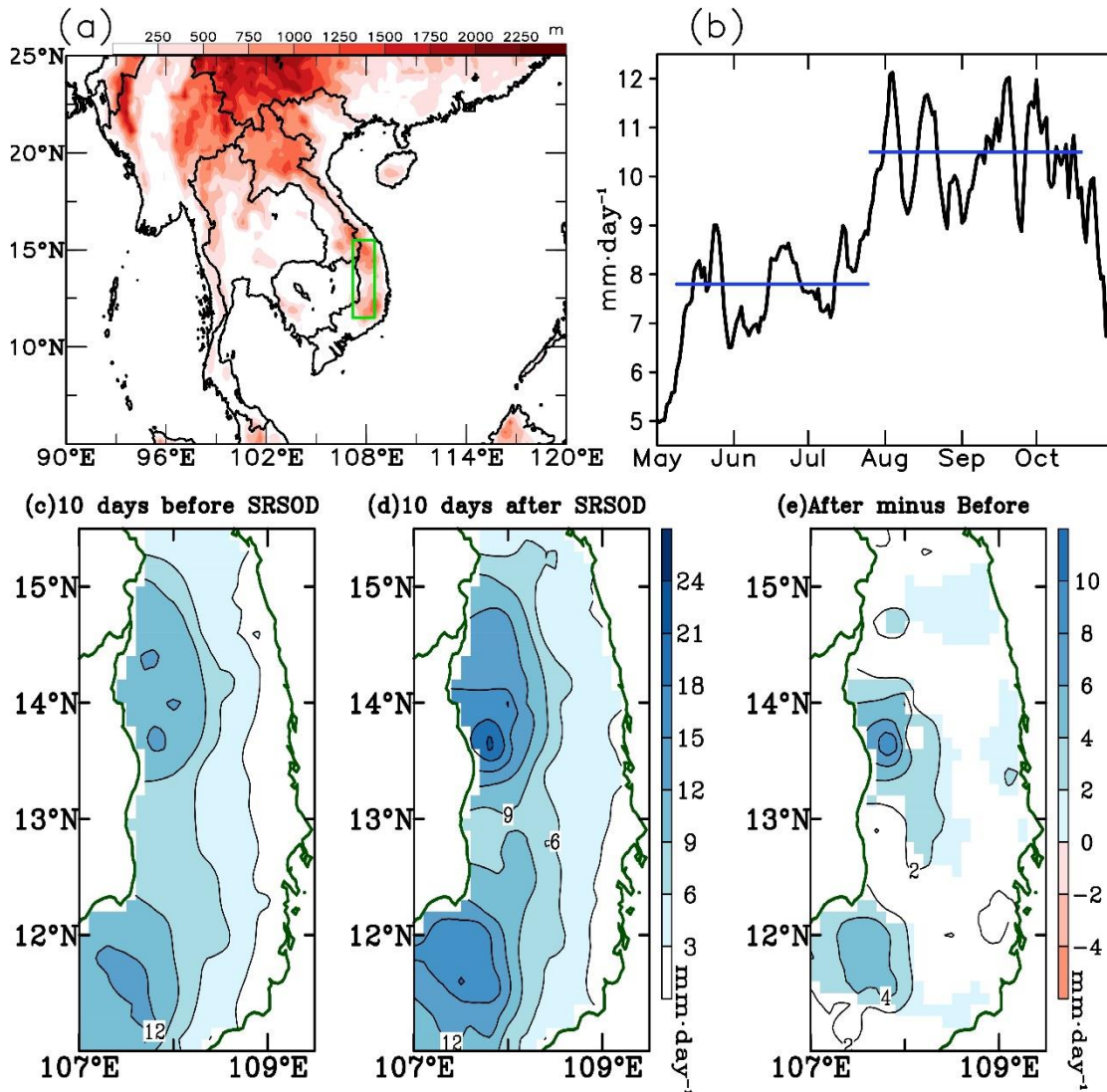
42 An abrupt increase in rainfall during the monsoon season in Asia could have a strong impact on
43 many activities of two thirds of the world's population, including agriculture, commerce,
44 forestry, and hydropower. Over Southeast Asia, rapid precipitation enhancement mainly occurs
45 during commencement of the Asian summer southwest monsoon, which signifies a transition
46 from the dry to the rainy season (Lau & Yang, 1997; Zhang et al., 2002; Nguyen-Le et al., 2015).
47 Therefore, research in past decades has increasingly focused on the summer monsoon onset date
48 (SMOD) or summer rainy season onset date (RSOD). For example, Zhang et al. (2002) used the
49 observed daily rainfall over the central Indochina Peninsula (ICP) to determine the mean SMOD
50 as being 9 May, with a standard deviation of 12 days. Applying the empirical orthogonal
51 function analysis on daily mean precipitation, Nguyen-Le et al. (2015) demonstrated that the
52 mean summer RSOD over the eastern ICP is 6 May, with a standard deviation of 13 days.
53 However, the immediate increase in rainfall over the eastern ICP is observed in early autumn
54 when the summer monsoon withdraws (Matsumoto, 1997; Yen et al., 2011; Chen et al., 2012;
55 Nguyen-Le et al., 2015).

56 Chen and Yoon (2000) demonstrated that the more (less) Indochina monsoon rainfall during cold
57 (warm) summers is the result of global divergent water vapor flux following interannual
58 variation in the global divergent circulation in response to tropical Pacific sea surface
59 temperature (SST) anomalies. Numerous efforts have been made to explore the relationship
60 between the interannual variation in monsoon onset and the El Niño Southern Oscillation

61 (ENSO). Years with cold (warm) SST anomalies in the equatorial central and eastern Pacific
62 Ocean in the preceding spring tend to have a stronger (weaker) monsoon circulation and an early
63 (late) SMOD and summer RSOD (Ju & Slingo, 1995; Zhang et al., 2002; Nguyen-Le et al.,
64 2015; Noska & Misra, 2016). As revealed by previous studies (e.g., Yen et al., 2011; Chen et al.,
65 2012), the maximum rainfall in coastal central Vietnam may undergo out-of-phase interannual
66 variation with the $\Delta\text{SST}(\text{Ni}\tilde{\text{n}}\text{o}3.4)$ index during October–November. However, Nguyen-Le et al.
67 (2015) illustrated that the mean autumn RSOD is 16 September, with a standard deviation of 12
68 days, and an early autumn RSOD was observed over the eastern ICP during the El Niño
69 development phase. Nevertheless, Nguyen et al. (2007) argued that the precipitation in a small
70 region of the Central Highlands (CH) of Vietnam is positively correlated with the equatorial
71 central to eastern Pacific SST from July to September but has no significant relationship with the
72 Indian Ocean SST.

73 The main coffee growing region of Vietnam, the second largest coffee producer worldwide
74 (Amarasinghe et al., 2015), is located over the CH (green box in Figure 1a). Moreover, the
75 hydropower potential generated from this region accounts for 25% of the country's total
76 hydropower potential (Dao & Bui, 2015). Because rainfall variation significantly influences
77 coffee production (Camargo, 2010) and hydropower potential, a thorough understanding of the
78 RSOD and SMOD over the CH is crucial to both Vietnam's agriculture and economy. By using
79 the same daily rainfall observations from 10 meteorological stations over the CH, Ngo-Thanh et
80 al. (2018) found that the RSOD and SMOD are well differentiated from each other, with the
81 mean RSOD being 20 April and SMOD being 13 May, whereas Pham-Thanh et al. (2020)
82 demonstrated that the average RSOD was 28 April, with a standard deviation of 14 days, and that
83 this was approximately 3 weeks before the mean SMOD in some years. Apart from the differing
84 RSODs due to different determination criteria between them, both studies reported a strong
85 correlation between the RSOD and the ENSO, but Pham-Thanh et al. (2020) reported most
86 RSODs being later (earlier) during El Niño (La Niña) phases.

87 As revealed from the 5-day-running-mean climatology of the rainfall index averaged over the
88 CH during May–October over the period 1983–2010 (Figure 1b), two distinct rainfall periods
89 emerge: the first period fluctuates along a rainfall of 7.8 mm day^{-1} and the second vacillates at
90 10.4 mm day^{-1} . Hereafter, these two rainy periods are referred to as the first rainy season (FRS)
91 and second rainy season (SRS), respectively. Studies related to rainfall over the CH have mostly
92 focused on the RSOD (equivalent to the FRS onset date here: FRSOD; Ngo-Thanh et al., 2018;
93 Pham-Thanh et al., 2020). To the best of our knowledge, this unique SRS feature and its onset
94 date (SRSOD) have not previously been explored. Therefore, in this study, we objectively
95 determine the SRSOD over the CH for the climatology as well as for each individual year during
96 1983–2010. In addition, the possible mechanism underlying the pronounced interannual variation
97 in SRSOD is investigated.



98
 99 **Figure 1.** (a) Topography; green box indicates the CH. (b) Daily climatology (5-day-running
 100 mean) of the rainfall index averaged over the CH during May–October over the period 1983–
 101 2010; the two blue lines indicate the mean rainfall during the FRS (9 May–25 July) and SRS
 102 (26 July–20 October), respectively. Mean rainfall over central Vietnam during the 10 days (c)
 103 before and (d) after the SRSOD, including the SRSOD, and (e) their differences. Shaded areas
 104 in (e) indicate significant differences above 90% confidence level.

105 2 Data and Methods

106 2.1 Datasets

107 To investigate the spatial and temporal characteristics of precipitation on a scale relevant to the
 108 climate over the CH, two types of consistent, long-term, high-resolution gridded rainfall dataset
 109 are acquired. The first is the Vietnam Gridded Precipitation (VnGP) dataset with a high
 110 resolution of $0.1^\circ \times 0.1^\circ$ and generated from 481 daily raingauge observations across all Vietnam
 111 over the period 1980–2010 (Nguyen-Xuan et al., 2016). We use this dataset to construct the
 112 rainfall indices and investigate the local rainfall variability over the CH. The second dataset used

113 is the daily Precipitation Estimation from Remotely Sensed Information using Artificial Neural
 114 Networks for Climate Data Record (PERSIANN-CDR), which has a resolution of $0.25^\circ \times 0.25^\circ$
 115 and is generated from long-term multisatellite high-resolution observations spanning 1983–2020
 116 (Ashouri et al., 2015). This dataset is used to examine the relationship between rainfall
 117 variability in the CH and the surrounding activity embedded in the large-scale environment. To
 118 depict the large-scale atmospheric circulation associated with the SRSOD, daily ERA-Interim
 119 reanalysis on a 0.75° latitude–longitude grid (Dee et al., 2011) is employed. Finally, the
 120 historical Oceanic Niño Index (ONI) provided by the Climate Prediction Center of National
 121 Centers for Environmental Prediction is adopted as a measure of the ENSO. For consistency,
 122 only the period 1983–2010 is covered in our analysis.

123 **2.2 Definition of the second rainy season onset date**

124 Because the SRS is a local feature in the CH and has not been observed in adjacent places,
 125 determination of the SRSOD by using only the rainfall parameter is proposed. In addition to the
 126 FRSOD and SRSOD, we designate RSRD and SRSRD as the rainy season retreat date and
 127 second rainy season retreat date, respectively. The procedures for detecting these four
 128 characteristic dates for the 28-year mean climatology are as follows:

- 129 1. FRSOD: The daily rainfall amount is larger than the yearly mean precipitation (PYRM) for 5
 130 consecutive days. And, there must be at least 10 days with daily rainfall amount larger than
 131 the PYRM within 20 consecutive days after the FRSOD.
- 132 2. RSRD: The same constraint as for the FRSOD is used to determine the RSRD, but the
 133 estimation is done backward from the year end.
- 134 3. SRSRD: The procedure is similar to that for the RSRD, but the average precipitation during
 135 the period FRSOD–RSRD (PRSM: the average rainfall over the entire rainy season) is
 136 considered instead of the PYRM and backward estimation is conducted starting from the date
 137 calculated as the RSRD minus 10 days.
- 138 4. SRSOD: The same procedure as that for the FRSOD is used, but the PYRM is replaced by
 139 the PRSM.

140 The first two procedures are similar to those reported by Ngo-Thanh et al. (2018) except that the
 141 PYRM over 28 years is considered instead of directly specifying 5 mm day^{-1} as a reference
 142 level.

143 First, both temporal variation and rainfall magnitude, as shown in Figure 1b, are greatly
 144 consistent with the ground-truth rainfall index illustrated in Figure 2 of Pham-Thanh et al.
 145 (2020), suggesting that the VnGP dataset is suitable for climate research related to the CH.
 146 Consequently, two distinct rainy periods (Figure 1b and Table 1) are defined: the first fluctuates
 147 along the average rainfall of 7.8 mm day^{-1} from 9 May to 25 July, whereas the second vacillates
 148 at 10.4 mm day^{-1} from 26 July to 20 October. To further substantiate the clear temporal
 149 development, the average rainfalls for both the 10 days before and after the SRSOD together
 150 with their differences are depicted in Figures 1c–1e. The significant increase in precipitation
 151 after the SRSOD implies that our procedure is capable of reasonably identifying the SRSOD and
 152 capturing the two separate rainfall stages, the FRS and SRS, over the CH.

154

155

Table 1. Various rainy season dates and related average rainfall statistics

rainfall unit: mm day ⁻¹					
Category	Climate		Early	Late	Normal
FRSOD	9 May		5 May	11 May	9 May
RSRD	21 Nov		5 Nov	27 Nov	28 Nov
SRSOD	26 Jul		7 Jul	19 Aug	26 Jul
SRSRD	20 Oct		7 Oct	22 Oct	4 Nov
Yearly rainfall average (PYRM)	5.7		5.9	5.6	5.7
Rainy season rainfall average (PRSM)	8.9		9.6	8.9	8.7
FRS rainfall average	7.8		7.1	7.6	7.7
SRS rainfall average	10.4		11.9	11.3	10.1
Onset date of the SRS over the CH from 1983 to 2010					
Year	SRSOD	Year	SRSOD	Year	SRSOD
1983	3 Aug	1993	26 Jul	2003	20 Jul
1984	27 Jul	1994	6 Jul	2004	23 Jul
1985	6 Aug	1995	19 Aug	2005	23 Jul
1986	15 Jul	1996	19 Jul	2006	29 Jun
1987	13 Aug	1997	10 Jul	2007	29 Jun
1988	11 Sep	1998	15 Aug	2008	22 Jul
1989	18 Jul	1999	23 Jul	2009	12 Jul
1990	13 Aug	2000	18 Aug	2010	22 Jul
1991	14 Aug	2001	3 Aug	Average	28 Jul

156

157 To reflect the apparent change in rainfall from the FRS to the SRS as well as the SRSOD
 158 identification for each individual year, many sensitivity tests are performed to eventually obtain
 159 the optimal criteria as follows. We first define some terms. P2SM denotes the average
 160 precipitation during 9 May–20 October, a fixed period based on the climatological FRSOD–
 161 SRSRD, for each individual year. PSA2 (PSB2) represents the average rainfall in the 20 days
 162 after (before) the SRSOD including (excluding) the SRSOD. The SRSOD of the CH is then
 163 determined by considering the first day after 27 June, just 1 month before 26 July of the
 164 climatological SRSOD, which satisfied the following conditions:

- 165 1. The 5-day-moving-averaged daily rainfall amount exceeds P2SM and persists for at least 5
 166 consecutive days.
- 167 2. PSA2 is greater than PSB2 + 0.35 × P2SM.

168 Consequently, the SRSODs for individual years during 1983–2010 are objectively determined
 169 (Table 1), and they exhibit clear interannual variation. The average SRSOD for 28 years is 28
 170 July, with a standard deviation of 17 days, whereas the earliest onset date is 29 June, occurred in
 171 2006 and 2007, and the latest onset date is 11 September, 1998.

172 **3 Results**

173 Because of the wide distribution of SRSODs, investigating any specific characteristics among
174 them is noteworthy. By using a standard deviation of ± 0.8 of the SRSOD over 28 years as a
175 measure, three discrete groups are selected and categorized as follows: early (1986, 1994, 1997,
176 2006, 2007, and 2009), late (1987, 1988, 1990, 1991, 1995, 1998, and 2000), and normal (other
177 years) SRS. Additionally, the first three procedures mentioned in Section 2.2 are applied to the
178 average rainfall index of each group to identify the FRSOD, RSRD, and SRSRD, whereas the
179 SRSOD is simply calculated as the average of each group's onset dates. According to the
180 statistics shown in Table 1 and Figure 2a, the early SRS years not only start earlier in terms of
181 the FRSOD and SRSOD and end earlier in terms of the RSRD and SRSRD but also have a
182 rainfall period 1 month longer than the late SRS years, along with higher precipitation in almost
183 every epoch except the FRS. Coincidentally, both the FRSOD and SRSOD in normal years are
184 identical to those in the 28-year climatology, with fewer rainfall differences for each rainy spell,
185 which suggests that the 28-year climate mean might nearly reach the climatic norm with the
186 exception of the RSRD and SRSRD. Although the FRSOD in each category is in early May,
187 Pham-Thanh et al. (2020) stated that an RSOD over the CH between late April and early May
188 seems to be more reasonable, not to mention using different criteria and datasets.

189 The intraseasonal oscillations (ISOs), including 10–20-day and 20–60-day modes, of the
190 observed rainfall in Vietnam have been well documented by Truong and Tuan (2018, 2019), but
191 these studies did not cover the CH. However, by using the VnGP dataset, Tuan (2019) found a
192 remarkable relationship between the rainfall submonthly scale ISO and heavy rainfall days in the
193 CH. Surprisingly, the SRSOD over the CH is synchronized with the developing phases of the
194 10–20-day and 20–60-day modes for each year in our study. Therefore, the original rainfall
195 indices and their respective filtered ISO modes plus the combined ISOs for all the selected years
196 in the aforementioned three groups are averaged with their center date coinciding with the
197 SRSOD and extending 30 days before and after, as illustrated in Figures 2b–2d. In general, the
198 precipitation clearly increases after the SRSOD in all three regimes, and the 10–20-day (20–60-
199 day) mode is more dominant in early (late) SRS years, whereas these two ISO modes are
200 compatible in the normal SRS years. These phenomena deserve extensive investigation in a
201 future study.

202 To further substantiate the precipitous rainfall development over the CH during the transition
203 from the FRS to the SRS, the composite rainfall, 28-year climate means with their center date
204 coinciding with the SRSOD, evolution (Figures 2e–2i), and differences between two consecutive
205 pentads (Figures 2j–2n) of pentad-mean VnGP (Text S1) are closely examined around the
206 SRSOD. The prominent rainfall enhancement after the SRSOD is confirmed by the delineated
207 physical domain with doubled rainfall intensity in Figure 2l if compared to that by the climate
208 mean in Figure 1e.

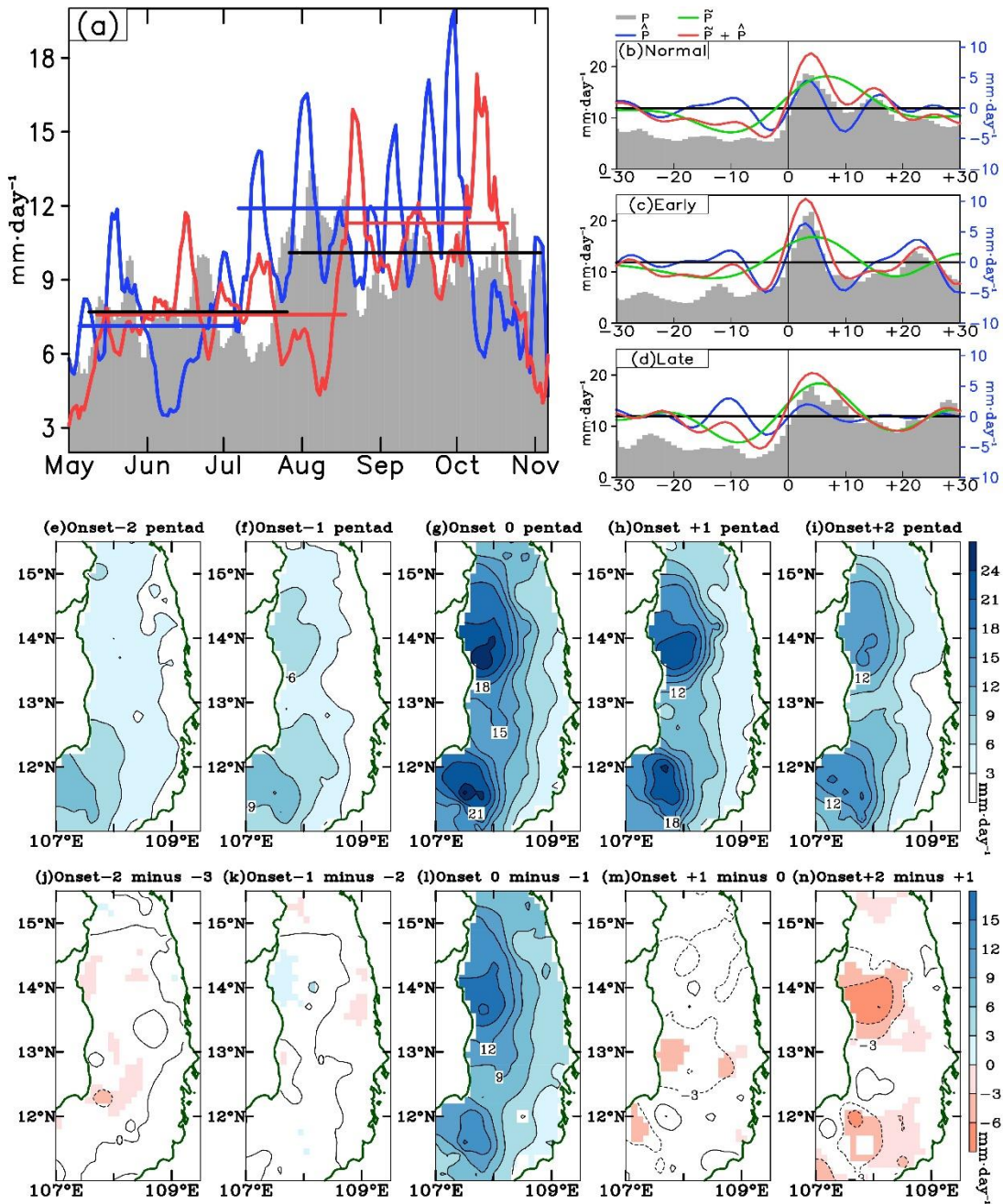


Figure 2. (a) Daily composite rainfall indices for normal (grey histogram), early (blue line), and late (red line) SRS years, respectively; two black, blue, and red horizontal lines indicate the rainfall mean during the FRS and the SRS for normal, early, and late SRS years, respectively. Daily evolution of composite P , \tilde{P} , \hat{P} , and $\tilde{P} + \hat{P}$ for (b) normal, (c) early, and (d) late SRS years; here \tilde{P} and \hat{P} represent the 20–60-day and 10–20-day modes, respectively. (e)–(i) Composite rainfall evolution and (j)–(n) differences between two consecutive pentads of pentad-mean VnGP over central Vietnam centered on the SRSOD. Shaded areas in (j)–(n) indicate a significant difference above 90% confidence level.

209
210
211
212
213
214
215
216
217

218

219 Regarding the conspicuous interannual variation in the SRSOD, July should be focalized on
220 considering its critical role of water vapor budget (Text S2) in differentiating between the early
221 and late SRS years because early (late) SRSODs occur in early July (until mid-August). The July
222 composite charts of (ψ_Q, Q_R, W) and (χ_Q, Q_D, P) for normal, early, and late SRS years are
223 displayed in Figures 3a–3f. In early SRS years, the abundant water vapor transported by strong
224 westerly winds over south-southeast Asia and the strengthened southeasterly wind over
225 northwestern Pacific (Text S3) is convergent toward the Philippine Sea west of 170°E and along
226 the trough in the south fringe of the Asian Monsoon Low, including the CH. Furthermore, the
227 significant increase in precipitation over these regions is accompanied and maintained by the
228 enhancement of convergent water vapor flux (Figure 3d). By contrast, the phenomenon in the
229 late SRS years associated with less vigorous water vapor transport and precipitation is similar to
230 that in the normal years. These arguments are illustrated further in Figures 3g–3l. A couple of
231 anomalous cyclonic cells of water vapor flux associated with the enhanced water vapor transport
232 stretch from north India toward the Philippine Sea west of 170°E, covering the CH (Figure 3g),
233 whereas the anomalous divergent water vapor flux $\Delta(\chi_Q, Q_D, P)$ converges water vapor toward
234 these regions to maintain excessive rainfall (Figure 3h) in early SRS years. Evidently, the
235 interannual rainfall variation in the CH is further ascertained by the composite rainfall
236 differences (Figures 3i and 3l), confirming the decisive role of July composite charts in
237 differentiating between early and late SRS years.

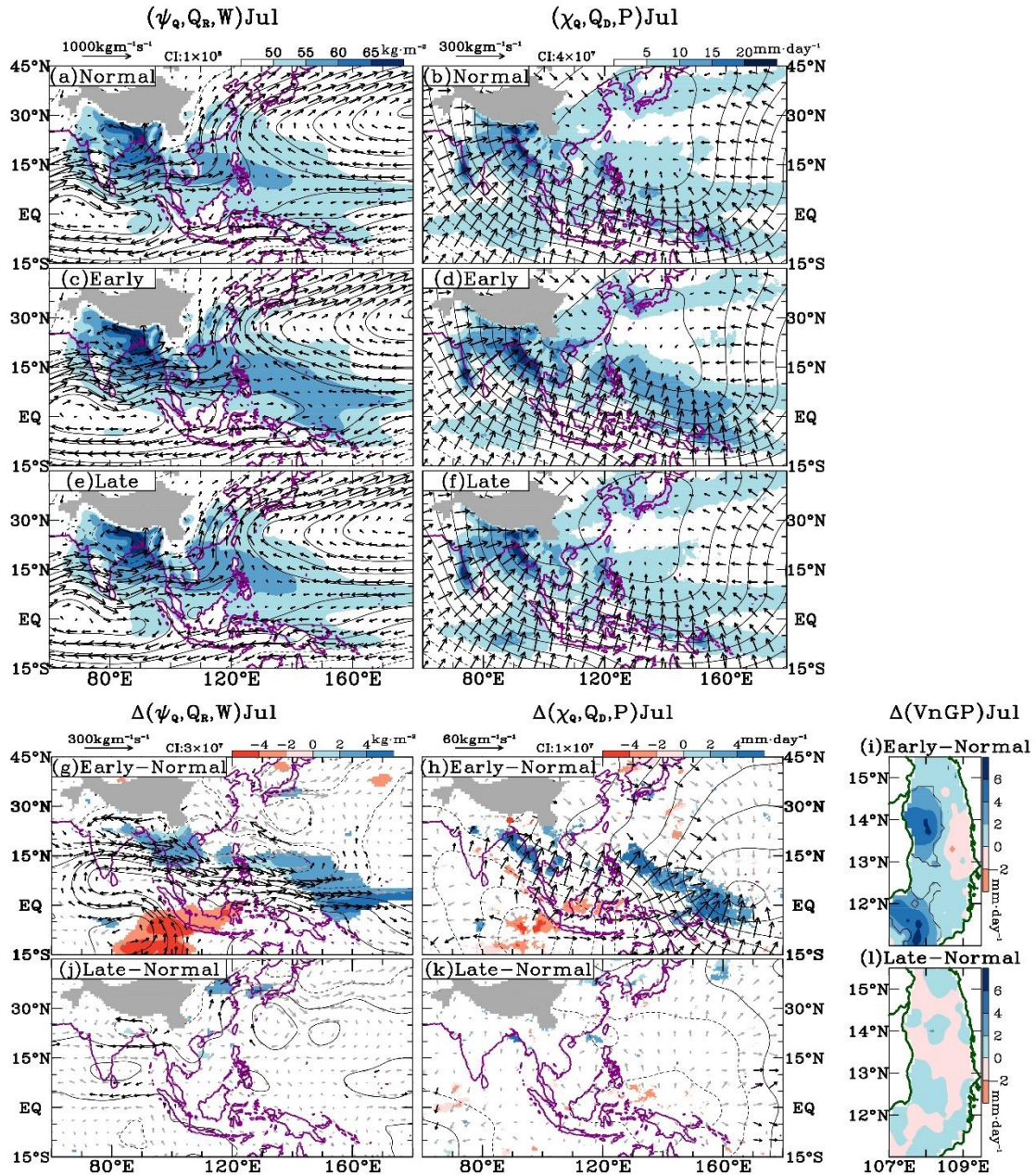
238 To explore the possible mechanism underlying the notable interannual variation in the SRSOD,
239 the time series of ONIs for each selected year in the early and late onset categories is displayed
240 in Figures 4a and 4b, respectively. Except for 2007, all early SRS years coincidentally occur
241 during El Niño developing phases, particularly with the Niño3.4 SST increase from January
242 through December. Because of the developing effect of the tropical storm Toraji in early July,
243 the persistent rainfall in the CH meets the SRSOD criteria despite the La Niña developing phase
244 in 2007. For late SRS years, the large-scale environment appears to be considerably diverse and
245 to comprise two El Niño (1987 and 1991), one normal (1990), one La Niña (2000), and three La
246 Niña developing phases (1988, 1995, and 1998). This discrepancy in diversification warrants
247 further investigation in the future.

248 An atypical Indian drought occurs during July 2002 with frequent advection of dry air from over
249 the deserts instead of marine moist air from the southern Indian Ocean (Bhat, 2006) despite 2002
250 being one of the El Niño developing phase years. Consequently, the drier water vapor transport
251 associated with divergence of water vapor flux replaces the moist large-scale environment over
252 the CH to hinder the expected early SRS occurrence. On the basis of the distinct result shown in
253 Figure 4a, the 5-year (except 2007) July composite chart of $\Delta(Q_D, SST)$ is constructed to support
254 the interannual rainfall variation outcomes depicted in Figures 3g–3i. From Figure 4c, we can
255 infer that the interannual variation in the divergent water vapor flux occurs in response to the
256 warmer July tropical Pacific SST anomalies to enhance the rainfall over the CH and eventually
257 induce early SRS onset.

258

259

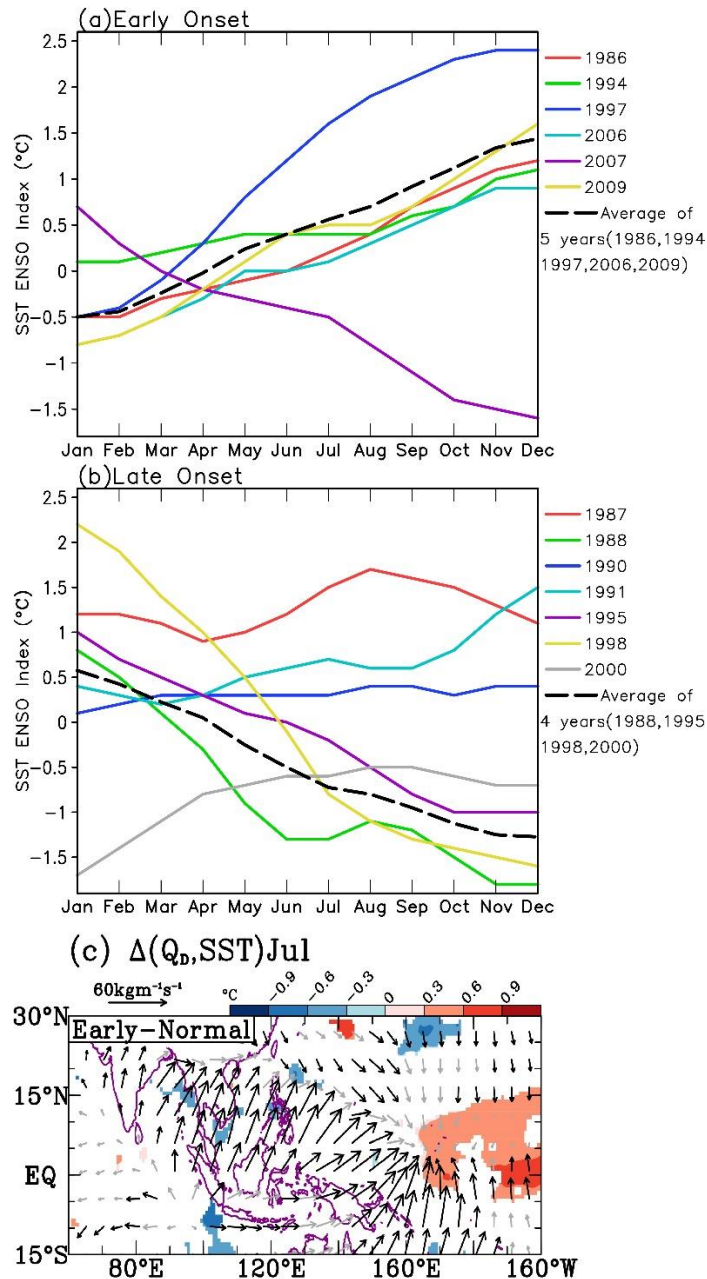
260



261
 262 **Figure 3.** July composite charts of ψ_Q (contour), Q_R (vector), and W (shaded) for (a) normal, (c)
 263 early, and (e) late SRS years, respectively. (b), (d), (f) Same as (a), (c), and (e) except for χ_Q
 264 (contour), Q_D (vector), and P (shaded). July composite charts of $\Delta(\psi_Q, Q_R, W)$ for (g) early and
 265 (j) late SRS years. (h), (k) Same as (g) and (j) except for $\Delta(\chi_Q, Q_D, P)$; shaded areas and black
 266 vectors in (g), (h), (j), and (k) denote a significant difference above 90% confidence level. (i),
 267 (l) Same as (h) and (k) except for $\Delta VnGP$; the areas that show a significant difference above
 268 90% confidence level in (i) and (l) are encircled by solid-black contour.

269

270



271
 272 **Figure 4.** (a) Monthly SST of the ENSO index for six early SRS years and average of five El
 273 Niño years. (b) Same as (a) except for seven late onset years and average of four La Niña
 274 years. (c) July composite chart of $\Delta(Q_D, SST)$ in five El Niño years. Shaded areas and black
 275 vectors in (c) denote a significant difference above 90% confidence level.

276 **4 Conclusions**

277 The CH is a climatological subregion in Vietnam, and the region is the major production for
 278 second largest coffee producer worldwide while also having a quarter of the total hydropower
 279 potential of the country. Therefore, rainfall variation may affect coffee production and
 280 hydropower potential, thereby directly affecting the agricultural and economic gross in the CH
 281 and the entire country. The findings of this study are summarized as follows: By using the VnGP

282 dataset for the 1983–2010 period, two distinct rainy periods in the CH are identified; the first
 283 fluctuates along the average rainfall of 7.8 mm day⁻¹ from 9 May (FRSOD) to 25 July, whereas
 284 the second vacillates at 10.4 mm day⁻¹ from 26 July (SRSOD) to 20 October (SRSRD).
 285 However, the prominent year-to-year variation in SRSOD leads to three separate regimes: an
 286 early (late) SRS occurring in early July (until mid-August) and a normal SRS starting in late
 287 July. The early SRS years are characterized by higher precipitation with a 1 month longer rainfall
 288 period than the late SRS years. Except for two unusual years (2002 and 2007) during 1983–2010,
 289 all the early SRS years occur during El Niño developing phases, particularly with the Niño3.4
 290 SST increase from January through December. The possible mechanism underlying the
 291 pronounced interannual variation in the SRSOD is inferred from water vapor budget analyses;
 292 the interannual variation in the divergent water vapor flux is in response to the warmer July
 293 tropical Pacific SST anomalies, resulting in rainfall intensification over the CH and eventually
 294 inducing early SRS onset.

295 **Acknowledgments and Data**

296 This study was supported by the Ministry of Science and Technology, Taiwan, under the grant
 297 MOST-108-2111-M-008-027. Data can be accessed online
 298 (VnGP:http://search.diasjp.net/en/dataset/VnGP_010; PERSIANN-
 299 CDR:<https://www.ncei.noaa.gov/data/precipitation-persiann/access/>; ERA-
 300 Interim:<https://apps.ecmwf.int/datasets/data/interim-full-daily/levtype=sfc>; ONI
 301 indices:https://origin.cpc.ncep.noaa.gov/products/analysis_monitoring/ensostuff/ONI_v5.php).

302 **References**

- 303 Amarasinghe, U. A., Hoanh, C. T., D’haeze, D., & Hung, T. Q. (2015). Toward sustainable
 304 coffee production in Vietnam: More coffee with less water. *Agricultural Systems*, 136, 96-
 305 105. <https://doi.org/10.1016/j.agsy.2015.02.008>
- 306 Ashouri, H., Hsu, K.-L., Sorooshian, S., Braithwaite, D. K., Knapp, K. R., Cecil, L. D., et al.
 307 (2015). PERSIANN-CDR: Daily precipitation climate data record from multisatellite
 308 observations for hydrological and climate studies. *Bulletin of the American Meteorological*
 309 *Society*, 96(1), 69-83. <https://doi.org/10.1175/BAMS-D-13-00068.1>
- 310 Bhat, G. S. (2006). The Indian drought of 2002 – a sub-seasonal phenomenon? *Quarterly*
 311 *Journal of the Royal Meteorological Society*, 132, 2583-2602. <https://doi.org/10.1256/qj.05.13>
- 312 Camargo, M. B. P. (2010). The impact of climatic variability and climate change on Arabic
 313 coffee crop in Brazil. *Bragantia*, 69, 239-247. [https://doi.org/10.1590/S0006-
 314 87052010000100030](https://doi.org/10.1590/S0006-87052010000100030)
- 315 Chen, T.-C. (1985). Global water vapor flux and maintenance during FGGE. *Monthly Weather*
 316 *Review*, 113, 1801–1819. [https://doi.org/10.1175/1520-0493\(1985\)113<1801:GWV FAM
 317 >2.0.CO;2](https://doi.org/10.1175/1520-0493(1985)113<1801:GWV FAM>2.0.CO;2)
- 318 Chen, T.-C., Tsay, J.-D., Yen, M.-C., & Matsumoto, J. (2012). Interannual variation of the late
 319 fall rainfall in central Vietnam. *Journal of Climate*, 25(1), 392-413.
 320 <https://doi.org/10.1175/JCLI-D-11-00068.1>
- 321 Chen, T.-C., & Yoon, J.-H. (2000). Interannual variation in Indochina summer monsoon
 322 rainfall: possible mechanism. *J. Climate*, 13(11), 1979-1986. [https://doi.org/10.1175/1520-
 323 0442\(2000\)013<1979:IVIISM>2.0.CO;2](https://doi.org/10.1175/1520-0442(2000)013<1979:IVIISM>2.0.CO;2)

- 324 Dao, N., & Bui, L. P. (2015). Rethinking Development Narratives of Hydropower in Vietnam. In
325 *Hydropower Development in the Mekong Region: Political, Socio-economic and*
326 *Environmental Perspectives*. (pp. 173-197). London: Earthscan.
- 327 Dee, D. P., Uppala, S., Simmons, A., Berrisford, P., Poli, P., Kobayashi, S., et al. (2011). The
328 ERA-Interim reanalysis: Configuration and performance of the data assimilation system.
329 *Quarterly Journal of the royal meteorological society*, *137*(656), 553-597.
330 <https://doi.org/10.1002/qj.828>
- 331 Ju, J., & Slingo, J. (1995). The Asian summer monsoon and ENSO. *Quarterly Journal of the*
332 *Royal Meteorological Society*, *121*(525), 1133-1168. <https://doi.org/10.1002/qj.49712152509>
- 333 Lau, K., & Yang, S. (1997). Climatology and interannual variability of the Southeast Asian
334 summer monsoon. *Advances in Atmospheric Sciences*, *14*(2), 141-162.
335 <https://doi.org/10.1007/s00376-997-0016-y>
- 336 Matsumoto, J. (1997). Seasonal transition of summer rainy season over Indochina and adjacent
337 monsoon region. *Advances in Atmospheric Sciences*, *14*(2), 231-245.
338 <https://doi.org/10.1007/s00376-997-0022-0>
- 339 Ngo-Thanh, H., Ngo-Duc, T., Nguyen-Hong, H., Baker, P., & Phan-Van, T. (2018). A
340 distinction between summer rainy season and summer monsoon season over the Central
341 Highlands of Vietnam. *Theoretical and applied climatology*, *132*, 1237-1246.
342 <https://doi.org/10.1007/s00704-017-2178-6>
- 343 Nguyen, T. D., Uvo, C., & Rosbjerg, D. (2007). Relationship between the tropical Pacific and
344 Indian Ocean sea-surface temperature and monthly precipitation over the central highlands,
345 Vietnam. *International Journal of Climatology*, *27*(11), 1439-1454.
346 <https://doi.org/10.1002/joc.1486>
- 347 Nguyen-Le, D., Matsumoto, J., & Ngo-Duc, T. (2015). Onset of the rainy seasons in the eastern
348 Indochina Peninsula. *Journal of Climate*, *28*(14), 5645-5666. [https://doi.org/10.1175/JCLI-D-](https://doi.org/10.1175/JCLI-D-14-00373.1)
349 [14-00373.1](https://doi.org/10.1175/JCLI-D-14-00373.1)
- 350 Nguyen-Xuan, T., Ngo-Duc, T., Kamimera, H., Trinh-Tuan, L., Matsumoto, J., Inoue, T., &
351 Phan-Van, T. (2016). The Vietnam Gridded Precipitation (VnGP) Dataset: Construction and
352 Validation. *SOLA*, *12*, 291-296. <https://doi.org/10.2151/sola.2016-057>
- 353 Noska, R., & Misra, V. (2016). Characterizing the onset and demise of the Indian summer
354 monsoon. *Geophysical Research Letters*, *43*, 4547-4554.
355 <https://doi.org/10.1002/2016GL068409>
- 356 Pham-Thanh, H., van der Linden, R., Ngo-Duc, T., Nguyen-Dang, Q., Fink, A. H., & Phan-Van,
357 T. (2020). Predictability of the rainy season onset date in Central Highlands of Vietnam.
358 *International Journal of Climatology*, *40*(6), 3072–3086. <https://doi.org/10.1002/joc.6383>
- 359 Truong, N. M., & Tuan, B. M. (2018). Large-scale patterns and possible mechanisms of 10–20-
360 day intra-seasonal oscillation of the observed rainfall in Vietnam. *International Journal of*
361 *Climatology*, *38*(10), 3801-3821. <https://doi.org/10.1002/joc.5534>
- 362 Truong, N. M., & Tuan, B. M. (2019). Structures and Mechanisms of 20-60 day intraseasonal
363 oscillation of the observed rainfall in Vietnam. *Journal of Climate*, *32*(16), 5191-5212.
364 <https://doi.org/10.1175/JCLI-D-18-0239.1>
- 365 Tuan, B. M. (2019). Extratropical forcing of submonthly variations of rainfall in Vietnam.
366 *Journal of Climate*, *32*(8), 2329-2348. <https://doi.org/10.1175/JCLI-D-18-0453.1>
- 367 Yen, M.-C., Chen, T.-C., Hu, H.-L., Tzeng, R.-Y., DINH, D. T., NGUYEN, T. T. T., & Wong,
368 C. J. (2011). Interannual variation of the fall rainfall in Central Vietnam. *Journal of the*
369 *Meteorological Society of Japan. Ser. II*, *89*, 259-270. <https://doi.org/10.2151/jmsj.2011-A16>

370 Zhang, Y., Li, T., Wang, B., & Wu, G. (2002). Onset of the summer monsoon over the Indochina
371 Peninsula: Climatology and interannual variations. *Journal of Climate*, 15(22),3206-3221.
372 [https://doi.org/10.1175/1520-0442\(2002\)015<3206:OOTSMO>2.0.CO;2](https://doi.org/10.1175/1520-0442(2002)015<3206:OOTSMO>2.0.CO;2)